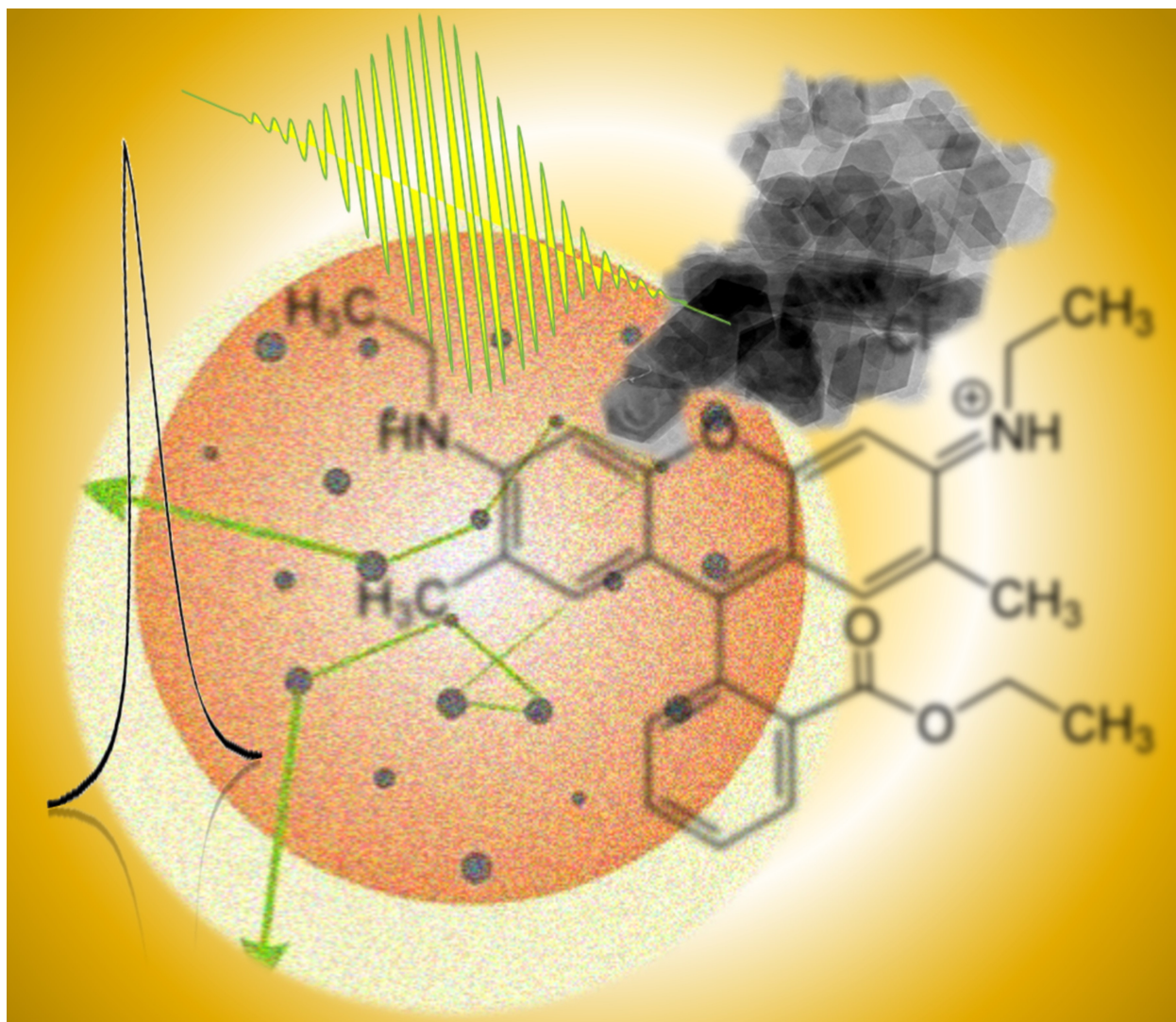


## Graphical Abstract

### Random lasing in Rhodamine 6G dye - Kaolinite nanoclay colloids under single shot nanosecond pumping

Nideesh Padiyakkuth, Rodolphe Antoine, Nandakumar Kalarikkal



## Highlights

### **Random lasing in Rhodamine 6G dye - Kaolinite nanoclay colloids under single shot nanosecond pumping**

Nideesh Padiyakkuth, Rodolphe Antoine, Nandakumar Kalarikkal

- Introduced Kaolinite nanoclay scatterers as a novel platform for colloidal Random lasers.
- Effect of concentration of gain and scatterers is studied in the context of line width narrowing and threshold behaviour.
- Narrowing and beta factors are calculated to quantify the disordered active system better.

# Random lasing in Rhodamine 6G dye - Kaolinite nanoclay colloids under single shot nanosecond pumping

Nideesh Padiyakkuth<sup>a</sup>, Rodolphe Antoine<sup>b</sup> and Nandakumar Kalarikkal<sup>a,c,d,\*</sup>

<sup>a</sup>School of Pure and Applied Physics, Mahatma Gandhi University, Kottayam-686 560, Kerala, India

<sup>b</sup>Institut Lumi'ere Mati'ere UMR 5306, Univ Lyon, Universit'e Claude Bernard Lyon 1, CNRS, F-69100 Villeurbanne, France

<sup>c</sup>International and Inter University Centre for Nanoscience and Nanotechnology, Mahatma Gandhi University, Kottayam 686560, Kerala, India

<sup>d</sup>School of Nanoscience and Nanotechnology, Mahatma Gandhi University, Kottayam 686 560, Kerala, India

## ARTICLE INFO

**Keywords:**  
Random lasers  
Kaolinite nanoclay  
Beta factor

## Abstract

Random lasers [RLs] are mirror-less light sources where feedback emanates from multiple scattering at the expense of spatial coherence and directionality. One of the most straightforward ways to build a random laser [RL] is by preparing a solution of a laser dye, which has a significantly large quantum yield with suspended scatterers (Colloidal based random lasers). Here we showed that rhodamine 6g (R6G) dye in methanol with Kaolinite nanoclay (scatterer) together could serve the purpose of a disordered active medium. It performs as a good novel platform for colloidal RLs. We investigated the dependence of the concentration of gain medium and scatterers in Kaolinite nanoclay colloidal RLs under single-shot nanosecond pumping. Line width narrows down to  $\approx 5$  nm above a threshold of  $40 \mu\text{J per pulse}$  for a particular concentration of gain and scatterer. Finally, narrowing and beta factors ( $\beta$ ) are also calculated for further quantification.


## 1. Introduction

Random lasers (RLs) are a particular class of optical devices where the optical feedback is provided by scattering rather than by an optical cavity as for traditional lasers [1]. The first random laser action in disordered systems was described by Letokhov [2, 3]. Then, H. Cao et al. have done Pioneering experimental developments in random laser devices [4]. Explorations of random lasers have been rapidly expanded, mainly because of their simplicity, underlying rich physics, applicability, and occurrence in a wide assortment of materials [5]. In general, RLs discover applications in sensors [6, 7, 8], display technology [9], homeland security [10], Photonic devices [11, 12], medical diagnostics [13, 14, 15, 16, 17], speckle free imaging [18, 19], random spectrometer on a chip [20] etc.

Typically, laser dyes are used as gain media in RLs due to their extraordinary photophysical properties. Such gain media should present very high quantum yield, photostability and a broad fluorescence spectrum proffering efficient gain. A combination of laser dye solution with scattering particles, liquid crystals, and various polymers can provide optical feedback. Such combination can induce laser-like emissions without any advanced fabrication technology, which is highly beneficial. A broad spectrum of materials has been employed to explore RL phenomena, including colloids [21], polymers [22], perovskites [23], random fiber lasers [24], semiconductor powders [25, 26], quantum dots [27, 28, 29]. In addition, metal nanoparticles (Au and Ag) are frequently used to improve the properties of RLs through surface plasmon-induced enhancements [30, 31, 32]. These colloidal systems are potentially applicable in photonics and can be integrated into devices based on tunable narrow-linewidth output. Although plethora of RL systems have been developing since last 15 years, developing novel nontoxic and sustainable composite nanomaterials for RLs is challenging.

Kaolinite nanoclay is a low-cost alternative and eco-friendly particles. Kaolinite (hydrous silicate) has a sheet-like structure with tetrahedral and octahedral sheets piled over one another. These sheets are constituent ingredients for clay layers assembled in different configurations. Kaolinite is discovered on the earth's surface and is an abundant clay mineral produced originally by the chemical weathering of igneous rocks comprising feldspar. The chemical composition of Kaolinite (hydrated Aluminium Silicate) is  $\text{Al}_2\text{Si}_2\text{O}_5(\text{OH})_4$  [33]. It was used as a diffusive material for light in incandescent bulbs, i.e. It should work as an excellent disordered system with a higher degree of scattering

\*Corresponding author,

 nkkalarikkal@mgu.ac.in (N. Kalarikkal)

ORCID(s):

strength. For avoiding coherent artefacts [34], it is common to use optical diffusers for speckle free imaging, and it has several applications in ceramics and refractories too. We calculated the  $\beta$  factor of the RL system. This work investigated the dependence of gain and scatterer concentration in Kaolinite nanoclay - R6G colloidal system for the random lasing application. We used nanoclay as passive scatterers, and R6G in methanol provides gain. This is the first report in which nanoclays are employed as scatterers to the best of our knowledge.

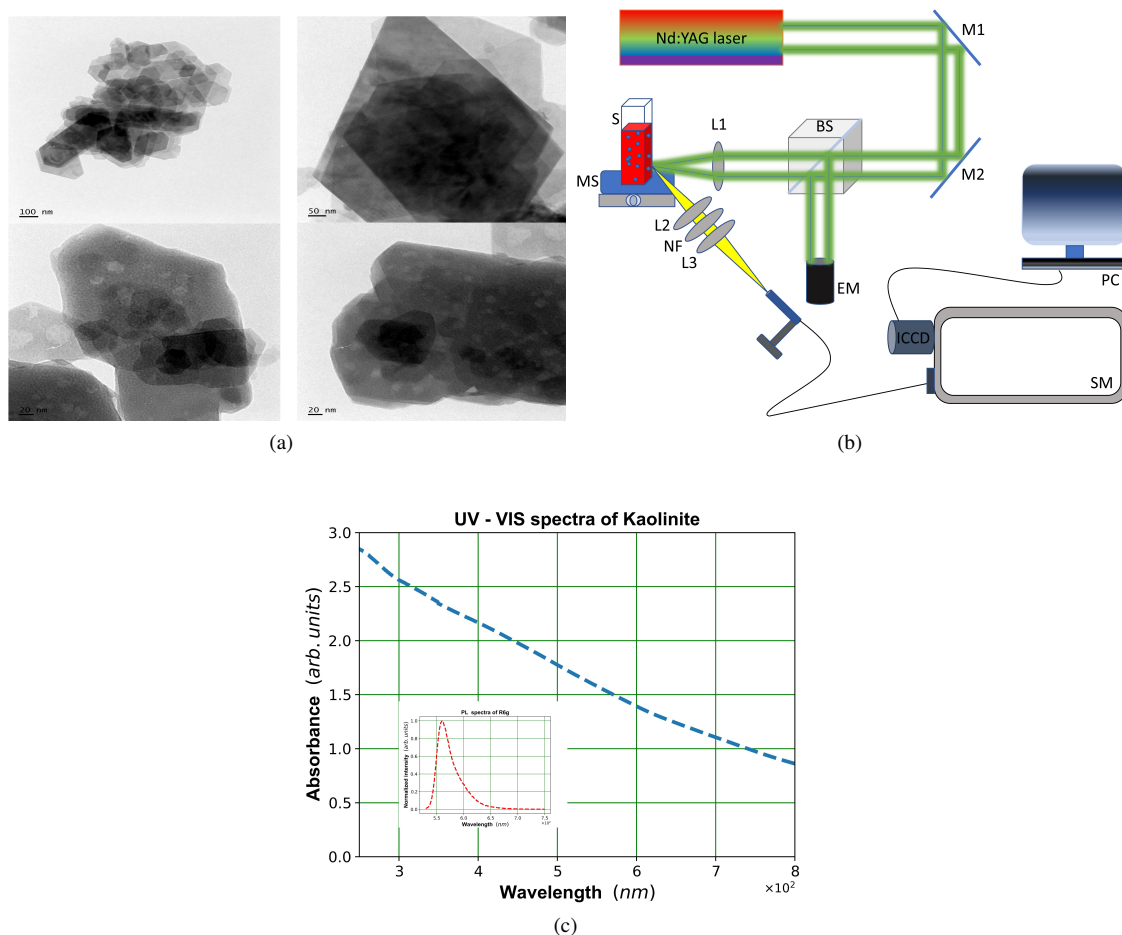


**Figure 1:** (a) Selected TEM images of Kaolinite nanoclay showing the morphology of the clays. (b) Experimental layout of the setup includes Nd:YAG laser, routing mirrors (M1 and M2), beam splitter (BS), lenses (L1, L2, and L3), notch filter (NF), sample (S), magnetic stirrer (MS), spectrometer (SM) and detector (ICCD). (c) UV-Vis extinction spectra of Kaolinite nanoclay (for optimal clay concentration used for RL experiment) and fluorescence spectrum of Rh6G (for optimal dye concentration used for RL experiment).

## 2. Sample preparation and experimental setup

### RL system:

The RL system comprises Kaolinite nanoclay as scatterers and R6G as the gain medium. Transmission electron microscopy [TEM] images focused on individual Kaolinite nanoclays are now presented in Fig 1a permitting us to address the clays' morphology better. TEM image of Kaolinite nanoclay shows that its average size is around 135 nm. Also, we conducted UV-Vis absorption measurements for clay concentration used for RL experiments (or, more precisely, extinction measurements). Therefore, the UV-Vis spectrum is presented in Fig 1c. Clearly, the long tail at high wavelengths is a signature of scattering provided by nanoclays. Clay minerals have an affinity towards cationic dyes, and consequently, we observed small adsorption for the clay-dye system. But such effect can be neglected by



**Table 1**

Values of different experimental parameters

Gain(mM)	Threshold energy ( $\mu\text{J per pulse}$ )	FWHM(nm)	NF	$\beta$
1	—	15	2.66	0.660
2	185	7	5.7	0.476
3	40	5	8	0.334
5	40	5	8	0.326

— cannot be accurately measured

**Table 2**

Values of different experimental parameters.

Scatterer (mg/ml)	Threshold energy ( $\mu\text{J per pulse}$ )	FWHM(nm)	NF	$\beta$
1	—	17	2.3	0.701
10	194	7	5.7	0.498
25	40	5	8	0.354

— cannot be accurately measured

adding sufficient gain concentration. Nanoclay and R6G are purchased from M/S EICL Ltd., Thiruvananthapuram, Kerala, India and Sigma Aldrich, respectively. All these materials were used without any further modification. We prepared two sets of samples, the first with a fixed amount of scatterers for different gain concentrations and the other with fixed gain for various scatterer concentrations. The required colloidal dye solution is synthesized by dissolving a specific amount of R6G (1 mM, 2 mM, 3 mM, and 5 mM) in methanol solution mixed with different amounts of Kaolinite nanoclay (1 mg/ml, 10 mg/ml, and 20 mg/ml).

### Experimental setup:

A Q-switched Nd: YAG laser laser operating at 1 Hz (externally triggered), 532 nm wavelength and 6 ns pulse duration were utilized as the excitation source for the gain medium. The experimental layout is shown in **Fig 1b**. For RL experiments, the beam was directed through a system of mirrors and focused on the sample employing a lens with a focal length of 10 cm (L1). The RL system is taken in a cuvette with 1 cm X 1 cm X 4 cm dimensions and is placed at 45 degrees with the direction of the incident beam. It is placed under a magnetic stirrer and continuously stirred to eliminate settling and ensure uniform scatterer dispersion throughout the experiment. Next, the RL emission is collected and focused on a fiber-coupled spectrometer (Andor SR - 500i spectrograph) using a collection optics (L2, notch filter, L3) set. Finally, the signal is detected using an intensified charge-coupled device (ICCD, Andor iStar). We thus performed single shot nanosecond spectral measurements for RL analysis.

### 3. Results and discussions

We observed lasing threshold behaviour, enhancement of intensity starting at that threshold, and line width narrowing for the Kaolinite-dye colloidal systems. We first realized the variation of peak intensity and FWHM (full width at half maximum) for different gain concentrations (1 mM, 2 mM, 3 mM, 5 mM) of R6G with a fixed amount of scattering particles (20 mg/ml). The output spectra from samples with disorders are similar to the fluorescence emission at all pump powers with only a difference in its line widths. In addition, the emission profile is consistently single-peaked with no apparent fluctuations in frequency. Line width decreases to  $\approx 5$  nm upon increasing the excitation energy from 10  $\mu\text{J}$  to 750  $\mu\text{J per pulse}$  for 3- and 5-mM gain concentrations. A critical initial dye concentration is needed for lasing to start with. Too low or too high concentration [35] will inhibit lasing phenomenon. The gain inside the system must beat the intrinsic losses to sustain lasing at the output. When the gain concentration increases, it is observed that the FWHM decreases tremendously at some point of input energy which is taken as the threshold as shown in **Fig 2 a - d**. Here in Fig 2 the red circles (left axis) indicate peak intensity and blue squares (right axis) represent (FWHM). The shaded region is to indicate the transition of slope at the threshold.

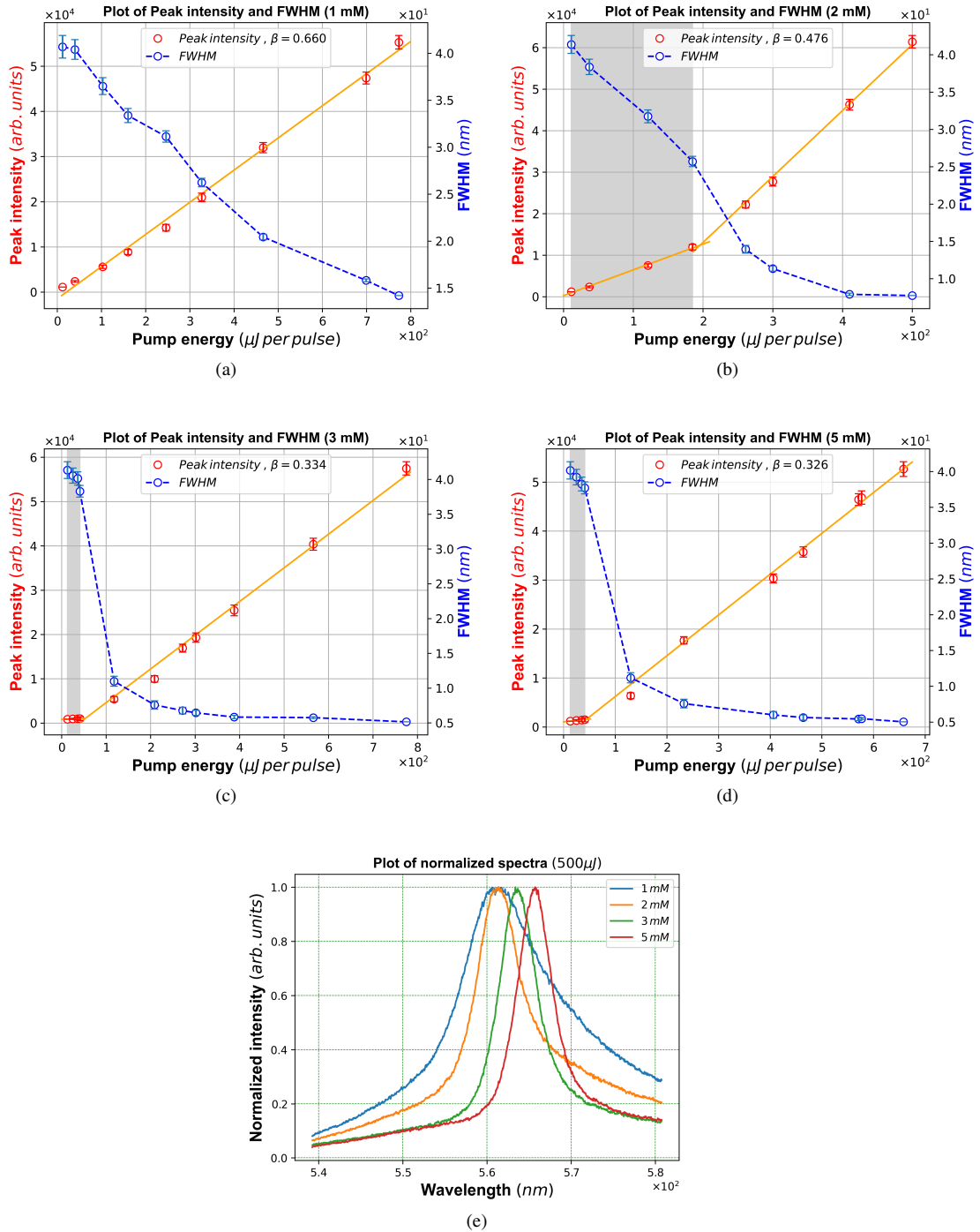


**Figure 2:** Variation of Peak intensity and FWHM with pump energy for gain concentrations 1mM, 2mM, 3mM, and 5mM in (a), (b), (c) and (d) respectively. (e) Plot of normalized intensity of the emission for different gain concentrations and fixed scatterer concentration.

The fluctuations in the mentioned parameters over 500 spectra are represented as error bars. A noticeable threshold activity cannot be witnessed in the 1 mM colloidal system because of insufficient gain. But by increasing from 2 mM

to 3 mM concentration, there is a significant change in the FWHM, thereby threshold energy since the gain tends towards optimum to surpass the loss and consequently achieved RL emission. Again, if we increase the gain, there

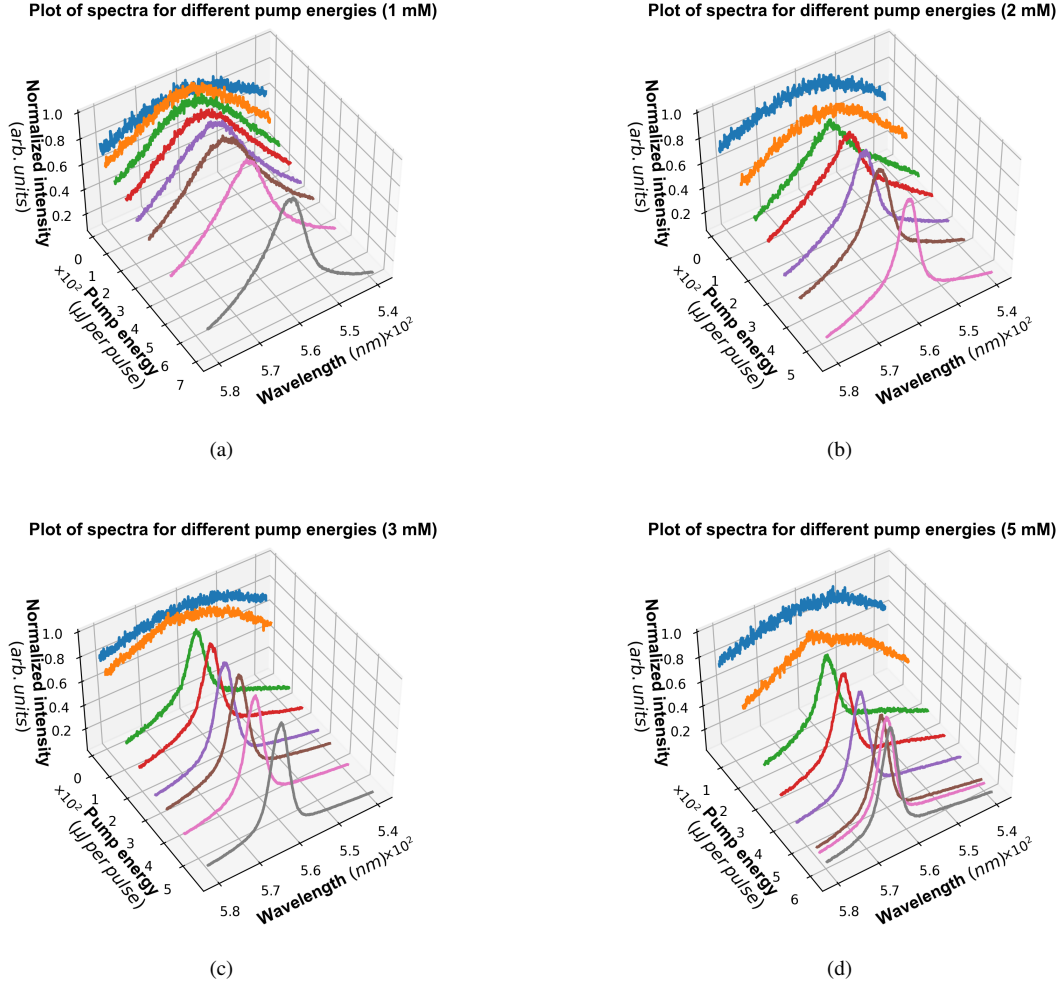


**Figure 3:** Emission spectra with different pump energy for gain concentrations 1 mM, 2 mM, 3 mM, 5 mM with 20 mg/ml scatterer concentration in (a), (b), (c), and (d) respectively.

is no significant change in the threshold and FWHM. In addition, Increasing the dye concentration affects the peak intensity of emission and the location of the wavelength that corresponds to the highest intense peak. That is reflected in the redshift of the wavelength. It can be attributed to the reabsorption and emission of unexcited R6G [36] as shown in **Fig 2e**. The corresponding threshold energy, FWHM, NF, and  $\beta$  factor is summarized in the **Table 1**. One of the important quantitative aspects of a random laser is its NF. It is the measure of gain narrowing and is defined as the ratio of FWHM below and far above the threshold [37, 38]. Typically, the emission has a line width of 40 nm (below threshold) and approximately 4 - 7 nm far above the threshold

$$NF = FWHM_{below} / FWHM_{above} \quad (1)$$

We have observed a gain narrowing by a factor of 8. Further, we also calculated the  $\beta$  factor and it decreases when the gain concentration increases. Typically, Spontaneous emission is the source for cavity lasing and in random lasers. Nevertheless, all spontaneous emissions don't partake in lasing. The portion of spontaneous emission that contributes to lasing output is comprehended as beta and lies between one and zero. The value of beta is directly related to the sharpness of the laser threshold. In conventional laser systems, the Beta value depends on the fraction of emitted

## Random lasing

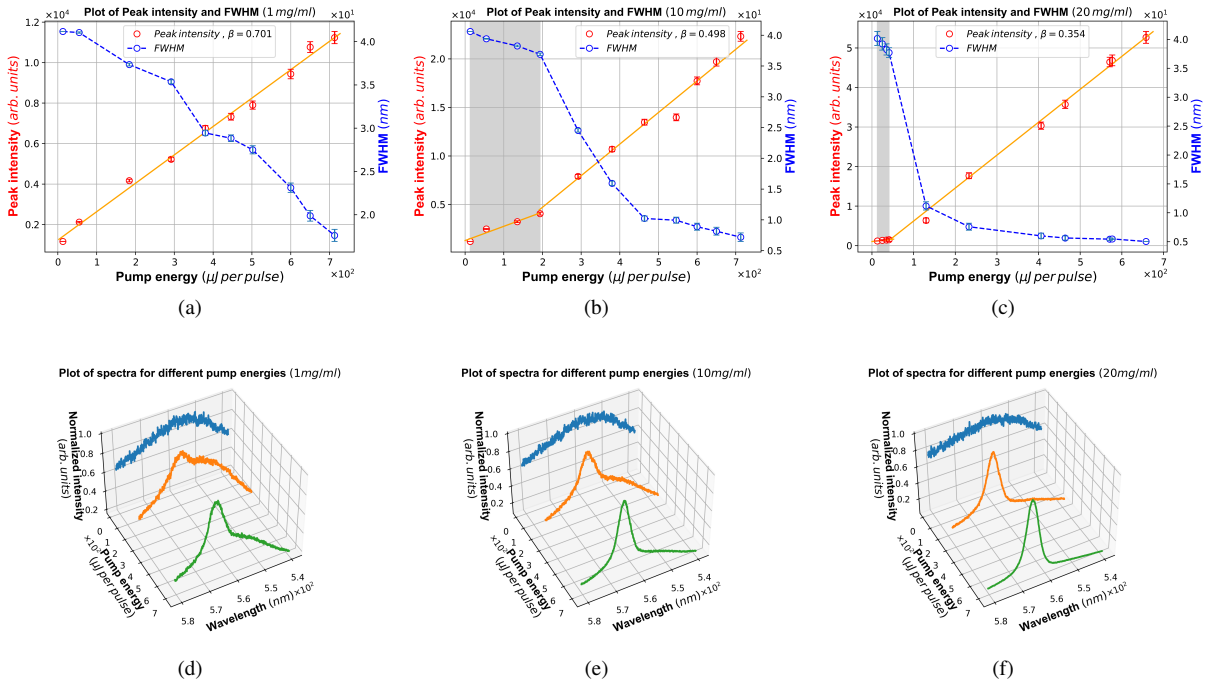


**Figure 4:** Behaviour of peak intensity and FWHM with pump energy for different scatterer concentration (1 mg/ml, 10 mg/ml, and 20 mg/ml) with 5 mM gain concentration in (a), (b), and (c) respectively. The corresponding emission spectra with different pump energy in (d)-(f).

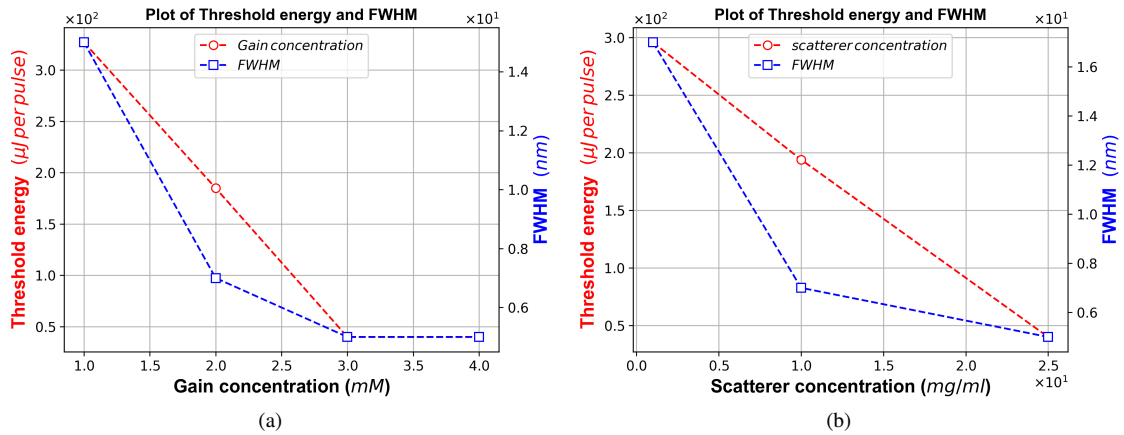


**Figure 5:** Dependence of threshold behaviour and FWHM with (a) gain concentration and (b) scatterer concentration.

photons collected by the mirrors and the fraction of spontaneous emission that overlaps with lasing spectra. But in RLs, it depends on the latter aspect only. Now, we can have three different cases. (i) When  $\beta = 1$ , every spontaneous photon will participate in lasing and will be threshold less. (ii) But if  $\beta = 0$ , the threshold will be very well defined and (iii) For  $0 < \beta < 1$ , the sharpness of the threshold becomes smaller as the value of  $\beta$  gets increases. The threshold power is defined as the value of the power where the slope of the curve ( $\beta = 0$ ) changes. Since the emission outside the narrowed spectrum cannot contribute to the lasing process, we use the overlap between below- and above-threshold emission spectra for defining beta. Thus, the beta value for RLs is relatively larger than conventional laser systems

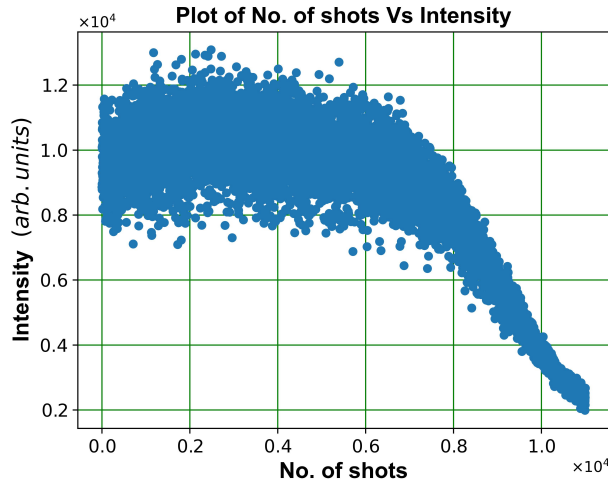


Figure 6: Photodegradation plot of RL sample

(between  $10^{-7}$  and  $10^{-10}$ ). Mathematically it is defined as

$$\beta = \int_{\lambda_0-\delta}^{\lambda_0+\delta} M(\lambda)L(\lambda) d\lambda \quad (2)$$

as proposed in the reference [39]. The recorded emission spectra for four different gain concentrations are represented in **Fig 3a-d**. Line width narrowing is evident in the spectra. Furthermore, line width decreases to different values above the threshold for different amounts of gain, as we discussed before. Since we got approximately 5 nm line width and a low threshold for 5 mM gain concentration. We selected that as an optimum gain and then studied the variation of threshold and FWHM with various scatterer concentrations.

**Fig 4a-c** indicated the response of peak intensity with the pump energy for 3 different scatterer concentrations with 5 mM R6G. for 1 mg/ml of Kaolinite nanoclay particle concentration, no reasonable change in the slope is observed, and that is obvious due to lower scattering strength. Line width decreases considerably ( $\approx 5$  nm) when we increase the amount of Kaolinite particles up to 20 mg/ml as depicted in **Fig 4b and c**. We increased the scatterer concentration from 1 mg/ml to 20 mg/ml and witnessed the lowering of FWHM, reduction of  $\beta$  factor and thereby, the threshold energy. The corresponding threshold energy, FWHM, NF, and  $\beta$  factor is summarized in the **Table 2**. The corresponding recorded emission spectra for 3 different scatterer concentrations are represented in **Fig 4d-f**. The lowering of threshold energy and FWHM with gain and scatterer concentration is even more evident from **Fig 5a and Fig 5b** respectively. Increasing the scattering strength will, in turn, improve the photon's dwell time inside the system and thereby, amplification occurs [40]. A drastic lowering of the  $\beta$  factor can also be observed while increasing the disorder, clearly indicating RL. In fact, few numbers of literature mention the beta values of RL systems. Such RL systems are dyes-doped with nanoparticles, perovskites, and liquid crystals. For optimal conditions, our beta factor is around 0.3 (see Tables 1 and 2), and the values reported in the literature range between  $\approx 0.1$ , and  $\approx 0.3$  [39, 41, 42, 43].

Long lifetimes and the capability of RL systems to work at higher repetition rates are pertinent properties for most RL applications [5]. Therefore, we conducted additional experiments with our RL system to better address these properties using an Nd: YAG laser (at 532 nm with a repetition rate of 10 Hz), and a pumping laser with energy far above the threshold. As a result, using the same colloidal protocol (as the one used with 1 Hz pumping laser experiments, **Fig 1b**), we obtained a quite long useful lifetime (the number of shots for which the emission intensity decreased to 50 % was 9270 laser shots, as depicted in **Fig 6**) which is a typical lifetime observed for other RL systems based on organic dyes and nanoparticles [44, 45].



## 4. Conclusion

In summary, we have introduced an RL system with Kaolinite nanoclay as scatterers in the R6G solution. We have investigated the dependence of gain and scatterer concentration in the context of line width narrowing and threshold behaviour. RL output is characterized by spectral narrowing and threshold behaviour with a reduction of the  $\beta$  factor. Scatterers' presence will increase the travel time of photons' inside the medium, and the optimal incorporation of gain synergetically result in random lasing. The narrowing and beta factors are measured and quantified to analyze the RL system better. Nanoclay - R6G colloidal system presents a new economically/ industrially viable - novel material for the random lasing applications.

## Acknowledgement

We acknowledge the financial support from BRNS-DAE-Govt. of India, DST-Govt. of India for funding through INSPIRE scheme, PURSE PI and PII, FIST and Nano Mission programs, UGC-Govt. of India for funding through SAP-DRS and Innovative program and SAIF-MGU. In addition, we acknowledge CNRS for funding through International Emerging Actions between Institut Lumière Matière, CNRS, France and Mahatma Gandhi University, India.

## CRedit authorship contribution statement

**Nideesh Padiyakkuth:** Term, Conceptualization, Methodology, Validation, Formal analysis, Investigation, Data curation. **Rodolphe Antoine:** Conceptualization, Methodology, Formal analysis, Data curation. **Nandakumar Kalarikkal:** Conceptualization, Methodology, Supervision, Funding acquisition.

## References

- [1] H. Cao, J. Xu, E. Seelig, R. Chang, Microlaser made of disordered media, *Applied Physics Letters* 76 (21) (2000) 2997–2999.
- [2] V. Letokhov, Generation of Light by a Scattering Medium with Negative Resonance Absorption, *Soviet Journal of Experimental and Theoretical Physics* 26 (4) (1968) 835.
- [3] R. Ambartsumyan, N. Basov, P. Kryukov, V. Letokhov, A laser with a nonresonant feedback, *IEEE J. Quantum Electron* 2 (9) (1966) 442–446.
- [4] H. Cao, Review on latest developments in random lasers with coherent feedback, *Journal of Physics A: Mathematical and General* 38 (49) (2005) 10497.
- [5] A. S. Gomes, A. L. Moura, C. B. de Araújo, E. P. Raposo, Recent advances and applications of random lasers and random fiber lasers, *Progress in Quantum Electronics* 78 (2021) 100343.
- [6] D. S. Wiersma, S. Cavalieri, A temperature-tunable random laser, *Nature* 414 (6865) (2001) 708–709.
- [7] M. Gaio, S. Caixeiro, B. Marelli, F. G. Omenetto, R. Sapienza, Gain-based mechanism for p h sensing based on random lasing, *Physical Review Applied* 7 (3) (2017) 034005.
- [8] W. Z. W. Ismail, G. Liu, K. Zhang, E. M. Goldys, J. M. Dawes, Dopamine sensing and measurement using threshold and spectral measurements in random lasers, *Optics express* 24 (2) (2016) A85–A91.
- [9] D. S. Wiersma, The physics and applications of random lasers, *Nature physics* 4 (5) (2008) 359–367.
- [10] X. Shi, W. Song, D. Guo, J. Tong, T. Zhai, Selectively visualizing the hidden modes in random lasers for secure communication, *Laser & Photonics Reviews* 15 (10) (2021) 2100295.
- [11] C.-Y. Su, C.-F. Hou, Y.-T. Hsu, H.-Y. Lin, Y.-M. Liao, T.-Y. Lin, Y.-F. Chen, Multifunctional random-laser smart inks, *ACS Applied Materials & Interfaces* 12 (43) (2020) 49122–49129.
- [12] A. Capocceffalo, E. Quintiero, M. Bianco, A. Zizzari, S. Gentilini, C. Conti, V. Arima, I. Viola, N. Ghofraniha, Random laser spectral fingerprinting of lithographed microstructures, *Advanced Materials Technologies* 6 (4) (2021) 2001037.
- [13] Q. Song, S. Xiao, Z. Xu, J. Liu, X. Sun, V. Drachev, V. M. Shalaev, O. Akkus, Y. L. Kim, Random lasing in bone tissue, *Optics letters* 35 (9) (2010) 1425–1427.
- [14] Y. Wang, Z. Duan, Z. Qiu, P. Zhang, J. Wu, D. Zhang, T. Xiang, Random lasing in human tissues embedded with organic dyes for cancer diagnosis, *Scientific reports* 7 (1) (2017) 1–7.
- [15] M. Hohmann, D. Dörner, F. Mehari, C. Chen, M. Späth, S. Müller, H. Albrecht, F. Klämpfl, M. Schmidt, Investigation of random lasing as a feedback mechanism for tissue differentiation during laser surgery, *Biomedical optics express* 10 (2) (2019) 807–816.
- [16] R. C. Polson, Z. V. Vardeny, Random lasing in human tissues, *Applied physics letters* 85 (7) (2004) 1289–1291.
- [17] Z. Xu, Q. Hong, K. Ge, X. Shi, X. Wang, J. Deng, Z. Zhou, T. Zhai, Random lasing from label-free living cells for rapid cytometry of apoptosis, *Nano letters* (2022).
- [18] B. Redding, M. A. Choma, H. Cao, Speckle-free laser imaging using random laser illumination, *Nature photonics* 6 (6) (2012) 355–359.
- [19] M. K. Bhuyan, A. Soleilhac, M. Somayaji, T. E. Itina, R. Antoine, R. Stoian, High fidelity visualization of multiscale dynamics of laser-induced bubbles in liquids containing gold nanoparticles, *Scientific Reports* 8 (1) (2018) 1–12.
- [20] B. Redding, S. F. Liew, R. Sarma, H. Cao, On-chip random spectrometer, in: *Applied Industrial Optics: Spectroscopy, Imaging and Metrology*, Optical Society of America, 2014, pp. AM2A–4.
- [21] N. M. Lawandy, R. Balachandran, A. Gomes, E. Sauvain, Laser action in strongly scattering media, *Nature* 368 (6470) (1994) 436–438.

- [22] S. Frolov, Z. Vardeny, K. Yoshino, A. Zakhidov, R. Baughman, Stimulated emission in high-gain organic media, *Physical Review B* 59 (8) (1999) R5284.
- [23] H.-W. Hu, G. Haider, Y.-M. Liao, P. K. Roy, R. Ravindranath, H.-T. Chang, C.-H. Lu, C.-Y. Tseng, T.-Y. Lin, W.-H. Shih, et al., Wrinkled 2d materials: A versatile platform for low-threshold stretchable random lasers, *Advanced Materials* 29 (43) (2017) 1703549.
- [24] S. Babin, A. El-Taher, P. Harper, E. Podivilov, S. Turitsyn, Tunable random fiber laser, *Physical Review A* 84 (2) (2011) 021805.
- [25] H. Cao, Y. Zhao, S. Ho, E. Seelig, Q. Wang, R. Chang, Random laser action in semiconductor powder, *Physical Review Letters* 82 (11) (1999) 2278.
- [26] J. Tian, G. Weng, Y. Wang, X. Hu, S. Chen, J. Chu, Random lasing in zno nanopowders based on multiphoton absorption for ultrafast upconversion application, *ACS Applied Nano Materials* 2 (4) (2019) 1909–1919.
- [27] Z. Xu, H. Zhang, C. Chen, G. Aziz, J. Zhang, X. Zhang, J. Deng, T. Zhai, X. Zhang, A silicon-based quantum dot random laser, *RSC Advances* 9 (49) (2019) 28642–28647.
- [28] Y. Chen, J. Herrnsdorf, B. Guilhabert, Y. Zhang, I. M. Watson, E. Gu, N. Laurand, M. D. Dawson, Colloidal quantum dot random laser, *Optics Express* 19 (4) (2011) 2996–3003.
- [29] Y. Wang, Y. Gao, V. Ta, H. V. Demir, H. Sun, Coherent random lasing from cdse/cds/zns quantum dots, in: *JSAP-OSA Joint Symposia*, Optical Society of America, 2013, p. 18p\_D5\_9.
- [30] X. Meng, K. Fujita, Y. Zong, S. Murai, K. Tanaka, Random lasers with coherent feedback from highly transparent polymer films embedded with silver nanoparticles, *Applied Physics Letters* 92 (20) (2008) 201112.
- [31] T. Zhai, Z. Xu, X. Wu, Y. Wang, F. Liu, X. Zhang, Ultra-thin plasmonic random lasers, *Optics express* 24 (1) (2016) 437–442.
- [32] K. Ge, D. Guo, X. Ma, Z. Xu, A. Hayat, S. Li, T. Zhai, Large-area biocompatible random laser for wearable applications, *Nanomaterials* 11 (7) (2021) 1809.
- [33] B. Zsirka, E. Horváth, É. Makó, R. Kurdi, J. Kristóf, Preparation and characterization of kaolinite nanostructures: reaction pathways, morphology and structural order, *Clay Minerals* 50 (3) (2015) 329–340.
- [34] S. Lowenthal, D. Joyeux, Speckle removal by a slowly moving diffuser associated with a motionless diffuser, *JOSA* 61 (7) (1971) 847–851.
- [35] K. Selanger, J. Falnes, T. Sikkeland, Fluorescence lifetime studies of rhodamine 6g in methanol, *The Journal of Physical Chemistry* 81 (20) (1977) 1960–1963.
- [36] C. Shu-Jing, S. Jin-Wei, Z. Tian-Rui, W. Zhao-Na, L. Da-He, C. Xiao, Wavelength variation of a random laser with concentration of a gain material, *Chinese Physics Letters* 28 (10) (2011) 104204.
- [37] G. Beckering, S. Zilker, D. Haarer, Spectral measurements of the emission from highly scattering gain media, *Optics letters* 22 (18) (1997) 1427–1429.
- [38] H. Cao, Lasing in random media, *Waves in random media* 13 (3) (2003) R1.
- [39] G. van Soest, A. Lagendijk,  $\beta$  factor in a random laser, *Physical Review E* 65 (4) (2002) 047601.
- [40] D. S. Wiersma, A. Lagendijk, Light diffusion with gain and random lasers, *Physical Review E* 54 (4) (1996) 4256.
- [41] S. Perumbilavil, A. Piccardi, O. Buchnev, M. Kauranen, G. Strangi, G. Assanto, All-optical guided-wave random laser in nematic liquid crystals, *Optics Express* 25 (5) (2017) 4672–4679.
- [42] Y.-H. Hong, T. S. Kao, Room-temperature random lasing of metal-halide perovskites via morphology-controlled synthesis, *Nanoscale Advances* 2 (12) (2020) 5833–5840.
- [43] A. Brito-Silva, A. Galembeck, A. S. Gomes, A. J. Jesus-Silva, C. B. de Araújo, Random laser action in dye solutions containing stöber silica nanoparticles, *Journal of Applied Physics* 108 (3) (2010) 033508.
- [44] P. I. Pincheira, A. F. Silva, S. I. Fewo, S. J. Carreño, A. L. Moura, E. P. Raposo, A. S. Gomes, C. B. de Araújo, Observation of photonic paramagnetic to spin-glass transition in a specially designed tio<sub>2</sub> particle-based dye-colloidal random laser, *Optics Letters* 41 (15) (2016) 3459–3462.
- [45] E. Jimenez-Villar, V. Mestre, P. C. de Oliveira, G. F. de Sa, Novel core–shell (tio<sub>2</sub>@ silica) nanoparticles for scattering medium in a random laser: higher efficiency, lower laser threshold and lower photodegradation, *Nanoscale* 5 (24) (2013) 12512–12517.